2008

Thorium-doping-induced superconductivity up to 56 K in Gd1-xThxFeAsO

Cao Wang
Zhejiang University, caow@uow.edu.au

Linjun Li
Zhejiang University

S Chi
Zhejiang University

Zeng-Wei Zhu
Zhejiang University

Zhi Ren
Zhejiang University

See next page for additional authors

http://ro.uow.edu.au/engpapers/5144

Authors

Cao Wang, Linjun Li, S Chi, Zeng-Wei Zhu, Zhi Ren, Yuke Li, Y T. Wang, Xiao Lin, Yongkang Luo, Shuai Jiang, Xiangfan Xu, Guanghan Cao, and Zhu-An Xu

Home   Search   Collections   Journals   About   Contact us   My IOPscience

Thorium-doping–induced superconductivity up to 56 K in Gd$_{1-x}$Th$_x$FeAsO

Thorium-doping–induced superconductivity up to 56 K in Gd$_{1-x}$Th$_x$FeAsO

CAO WANG, LINJUN LI, SHUN CHI, ZENGWEI ZHU, ZHI REN, YUKE LI, YUETAO WANG, XIAO LIN, YONGKANG LUO, SHUAI JIANG, XIANGFAN XU, GUANGHAN CAO[(a)] and ZHU'AN XU[(b)]

Department of Physics, Zhejiang University - Hangzhou 310027, People's Republic of China

Abstract – We report a new strategy to induce superconductivity in iron-based oxyarsenide. Instead of F$^-$ substitution for O^{2-}, we employed Th^{4+} doping in GdFeAsO with the consideration of "lattice match" between Gd$_2$O$_2$ layers and Fe$_2$As$_2$ ones. As a result, superconductivity with T_c^{onset} as high as 56 K was realized in a Gd$_{0.8}$Th$_{0.2}$FeAsO polycrystalline sample. This T_c value is among the highest ever discovered in the iron-based oxypnictides.

Introduction. – Following the discovery of superconductivity in an iron-based arsenide LaO$_{1-x}$F$_x$FeAs with a superconducting transition temperature (T_c) of 26 K [1], T_c was pushed up surprisingly to above 40 K by either applying pressure [2] or replacing La with Sm [3], Ce [4], Nd [5] and Pr [6]. The maximum T_c^{onset} has climbed to 55 K, observed in SmO$_{1-x}$F$_x$FeAs [7,8] and SmFeAsO$_{1-x}$ [9]. The value of T_c was found to increase with decreasing lattice parameters in LnFeAsO$_{1-x}$F$_x$ (Ln stands for the lanthanide elements) at an apparently optimal doping level. However, the F$^-$ doping in GdFeAsO (whose lattice constants are the smallest) produced T_c only below 40 K [10,11].

The LnFeAsO family [12] crystallizes in a tetragonal ZrCuSiAs-type [13] structure with space group *P4/nmm*. From the crystal chemistry point of view, the crystal structure can be described as an alternate stacking of Ln$_2$O$_2$ fluorite-type block layers and Fe$_2$As$_2$ antifluorite-type block layers along the *c*-axis. The two block layers are connected by CsCl-type layers (see fig. 1). Therefore, the chemical stability of LnFeAsO depends, to some extent, on the lattice match between the two block layers. A rough estimate based on the effective ionic radii [14] indicates that the Ln$_2$O$_2$ planar lattice is substantially smaller than the Fe$_2$As$_2$ lattice. The layer mismatch becomes more significant for the LnFeAsO member with a smaller
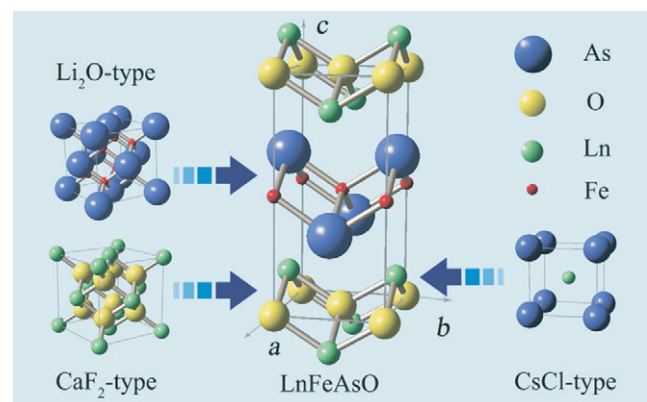

Fig. 1: Crystal chemistry understanding of the structure of LnFeAsO (Ln = lanthanides). The stacking of fluorite (CaF$_2$) layers, CsCl-type layers and antifluorite (Li$_2$O) layers along the *c*-axis forms the LnFeAsO structure. The lattice constant along the stacking direction can be expressed by the formula $c \simeq \frac{1}{2}a_{CaF_2} + \frac{1}{2}a_{CsCl} + \frac{1}{2}a_{Li_2O}$, which basically satisfies the experimental results. Note that the lattice match between the Ln$_2$O$_2$ layers and the Fe$_2$As$_2$ layers affects the chemical stability of LnFeAsO.

Ln^{3+} ion. This may explain why TbFeAsO, DyFeAsO and other heavy-lanthanide–containing LnFeAsO members were hard to synthesize previously [12].

As the family member with the relatively small Ln^{3+} ion, GdFeAsO is a promising parent compound to have a

[(a)]E-mail: `ghcao@zju.edu.cn`
[(b)]E-mail: `zhuan@zju.edu.cn`

higher T_c through carrier doping. Similar to cuprate superconductors in which superconductivity emerges when charge carriers are induced into CuO_2 planes by chemical doping at "charge reservoir layers" [15], superconductivity in $LnFeAsO_{1-x}F_x$ is realized by partial substitution of O^{2-} with F^-. The F^--for-O^{2-} substitution introduces extra positive charges in the insulating Ln_2O_2 layers and negative charges (electron doping) in the Fe_2As_2 layers. An earlier preliminary experiment showed signs of superconductivity below $10\,K$ in $GdFeAsO_{1-x}F_x$ [10]. Later, T_c was pushed up to $36\,K$ in a polycrystalline sample with a nominal composition of $GdO_{0.83}F_{0.17}FeAs$ [11]. Very recently the T_c value was increased to $53.5\,K$ in oxygen-deficient $GdFeAsO_{1-x}$ by using high-pressure synthesis [16]. It is of great interest whether the T_c can be elevated further in electron-doped $GdFeAsO$ systems.

Up to now, electron doping in the iron-based oxyarsenides was realized through the chemical substitution only at the oxygen site in Ln_2O_2 layers (it is here noted that hole doping in $La_{1-x}Sr_xFeAsO$ system, which was reported to show superconductivity at $25\,K$, was on the La-site [17]). Because the ionic radius of F^- ($1.31\,\text{\AA}$, $CN = 4$) is distinctly smaller than that of O^{2-} ($1.38\,\text{\AA}$, $CN = 4$) [14], F^- substitution for O^{2-} in $GdFeAsO$ leads to more severe lattice mismatch as mentioned above. In other words, doping F^- (or oxygen vacancy) in $GdFeAsO$ is particularly difficult, which is probably the main obstacle to elevate T_c. Substitution of Ln^{3+} by relatively large tetravalence ions is an alternative route to introduce electrons. A successful example was the electron doping in $Ln_{2-x}Ce_xCuO_4$ ($Ln = Pr$, Nd or Sm), which has led to the discovery of n-type cuprate superconductors [18]. Th^{4+} is a very stable tetravalence ions and is as large as Gd^{3+} [14], therefore, we pursued the Th^{4+} substitution for Gd^{3+} in the $GdFeAsO$ system.

Experimental. – Polycrystalline samples of $Gd_{1-x}Th_xFeAsO$ were synthesized by a solid state reaction in an evacuated quartz tube. All the starting materials (Gd, Gd_2O_3, ThO_2, Fe and As) are with high purity ($\geqslant 99.95\%$). First, GdAs was presynthesized by reacting Gd tapes with As pieces in vacuum at $773\,K$ for 10 hours and then at $1173\,K$ for 12 hours. Similarly, FeAs was prepared by reacting Fe powders with As shots at $773\,K$ for 6 hours and then at $1030\,K$ for 12 hours. Then, powders of GdAs, Gd_2O_3, ThO_2, Fe and FeAs were weighed according to the stoichiometric ratio of $Gd_{1-x}Th_xFeAsO$. The weighed powders were mixed thoroughly by grinding, and pressed into pellets under a pressure of $4000\,kg/cm^2$ in an argon-filled glove box. The pressed pellets were wrapped with Ta foils, and sealed in an evacuated quartz ampoule. The sealed ampoule was slowly heated to $1423\,K$, holding for 48 hours. Finally the samples were rapidly cooled to room temperature.

Powder X-ray diffraction was performed at room temperature using a D/Max-rA diffractometer with Cu
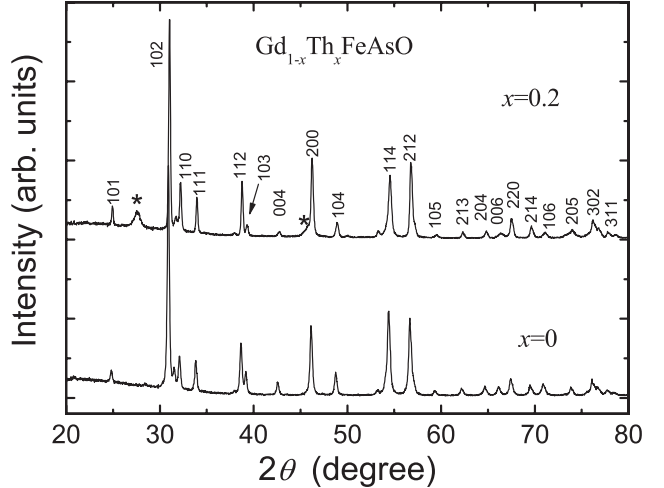

Fig. 2: Powder XRD of $Gd_{1-x}Th_xFeAsO$ polycrystalline samples. The asterisked peaks come from unreacted ThO_2.

K_α radiation and a graphite monochromator. The XRD diffractometer system was calibrated using standard Si powder. Lattice parameters were refined by a least-squares fit using at least 20 XRD peaks. Energy-dispersive X-ray (EDX) spectra were obtained by using the Phoenix EDAX equipment attached to a field-emission scanning electron microscope (SIRION FEI). The ground sample powder was placed directly on the copper sample holder for making the SEM specimen.

The electrical resistivity was measured with a standard four-terminal method. Samples were cut into a thin bar with typical size of $4\,mm \times 2\,mm \times 0.5\,mm$. Gold wires were attached onto the samples' newly abraded surface with silver paint. The size of the contact pads leads to a total uncertainty in the absolute values of resistivity of 10%. The electrical resistance was measured using a steady current of $5\,mA$, after checking the linear I-V characteristic.

Temperature dependence of magnetization was measured on a Quantum Design Magnetic Property Measurement System (MPMS-5). For the measurement of the undoped compound, the applied field was $1000\,Oe$. For the measurement of the Th-doped superconducting samples, both the zero-field-cooling and field-cooling protocols were employed under the field of $10\,Oe$.

Results and discussion. – Figure 2 shows the X-ray diffraction (XRD) patterns of the $Gd_{1-x}Th_xFeAsO$ samples. The XRD peaks of the undoped compound can be well indexed based on the tetragonal ZrCuSiAs-type structure, indicating single phase of $GdFeAsO$. As for the Th-doped samples, small amount of unreacted ThO_2 can be seen. The refined lattice parameters are $a = 3.9154(2)\,\text{\AA}$ and $c = 8.4472(4)\,\text{\AA}$ for the parent compound, basically consistent with the previously reported values [12]. For the Th-doped sample of $x = 0.2$, the fitted lattice parameters are $a = 3.9161(2)\,\text{\AA}$ and $c = 8.4386(3)\,\text{\AA}$. Therefore,
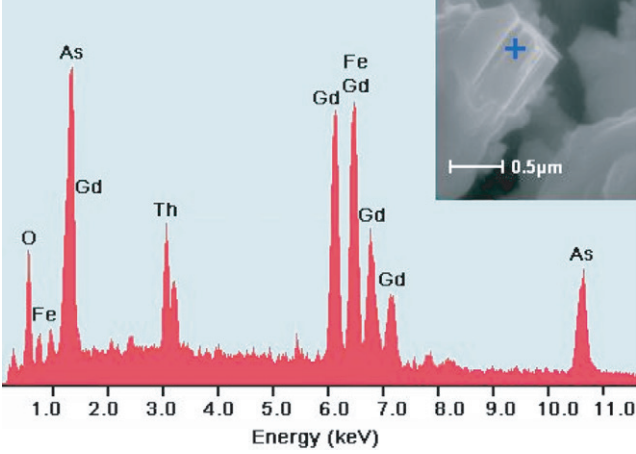
Fig. 3: A representative EDX spectrum of a crystalline grain of $Gd_{0.8}Th_{0.2}FeAsO$ sample, indicating the incorporation of thorium into the lattice. The inset shows the SEM image of the same sample. The marked spot is the position where the EDX spectrum was collected.

Fig. 4: Temperature dependence of electrical resistivity (ρ) in $Gd_{1-x}Th_xFeAsO$. The data are normalized to $\rho_{300\,K}$ as the resistivity measured on polycrystalline samples is often higher than the intrinsic value due to the grain boundary and surface effect. The inset is an expanded plot to show the superconducting transition at 56 K for the sample of $x = 0.2$.

Fig. 5: Temperature dependence of magnetic susceptibility (χ) of $Gd_{1-x}Th_xFeAsO$. The lower inset shows the differential χ_{FC} curve of $Gd_{0.8}Th_{0.2}FeAsO$ powder sample, which locates the T_c^{onset} at 56.3 K. ZFC, zero-field cooling; FC, field cooling.

though the a-axis almost remains unchanged, the c-axis is shorten significantly by the Th-doping, indicating that thorium is indeed incorporated into the lattice. The shrinkage of the c-axis is attributed to the strengthening of the interlayer Coulomb attraction as a consequence of Th^{4+} doping.

More direct evidence of Th incorporation into the lattice comes from the chemical composition measurement by energy-dispersive X-ray (EDX) microanalysis. Figure 3 shows that the microcrystal in the SEM image contains remarkably Th in addition to Gd, O, Fe and As. Quantitative analysis gives the Gd : Th : Fe : As ratios as $0.83 : 0.19 : 0.96 : 1.00$ for the $x = 0.2$ sample (here we omit the oxygen content because the amount of oxygen cannot be measured so precisely by EDX technique). This result demonstrates that most of the Th was successfully doped for the sample of $x = 0.2$.

Figure 4 shows the $\rho(T)$ curve for $Gd_{1-x}Th_xFeAsO$ samples. For the undoped $GdFeAsO$, the $\rho(T)$ curve exhibits an obvious anomaly at 135 K, characterized by a resistivity drop with decreasing temperature. In $LaFeAsO$ a similar resistivity anomaly was found at 150 K [1,19] which has been recently suggested to be associated with a structural phase transition and/or an antiferromagnetic spin-density-wave transition [19–21]. We speculate that the present resistivity anomaly in $GdFeAsO$ has a similar physical origin with that in $LaFeAsO$. For $x = 0.2$ such resistivity anomaly disappears, instead, resistivity drops abruptly to zero below 56 K, indicating a superconducting transition. In addition, the linear temperature-dependence of normal-state resistivity near T_c suggests possible non-Fermi liquid behavior in the present system, similar to that in $SmFeAsO_{1-x}F_x$ [8].

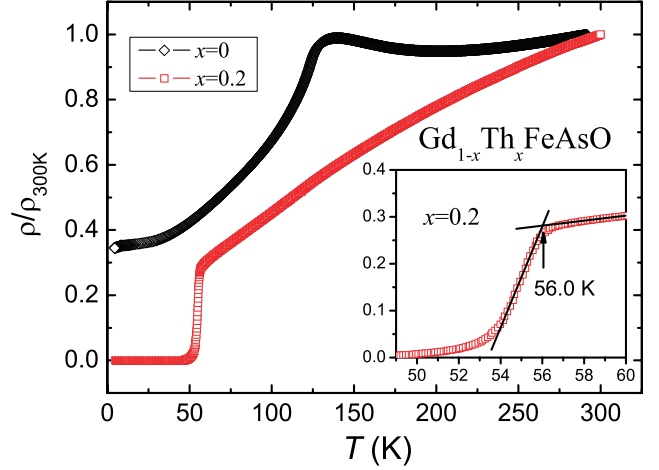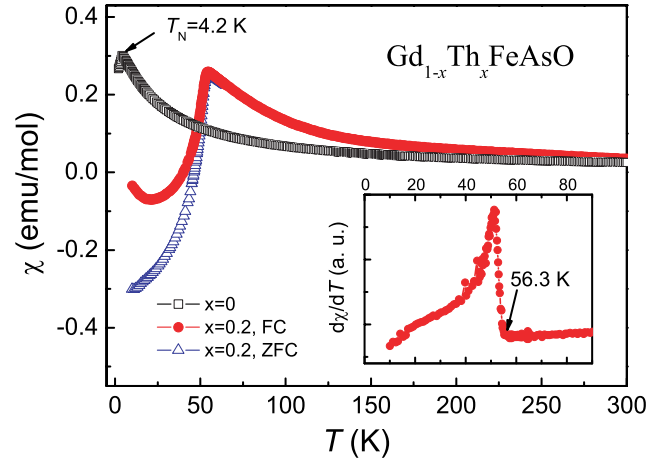The magnetic measurement on $Gd_{1-x}Th_xFeAsO$ samples was shown in fig. 5. The high-temperature

magnetic susceptibility (χ) of the parent compound follows the Curie-Weiss law. The fitted effective magnetic moment was $7.96\,\mu_B$ per formula unit, in good agreement with the magnetic moment of a free Gd^{3+} ion. Below 4.2 K, χ drops sharply, indicating an antiferromagnetic ordering of Gd^{3+} magnetic moments. Note that similar behavior was observed in $SmFeAsO$, where the Neel temperature was 4.6 K [22].

For the Th-doped samples, the normal-state susceptibility roughly obeys the Curie-Weiss law. Below 55 K, χ drops steeply to negative values, confirming the superconductivity observed above. After subtracting the paramagnetic susceptibility of Gd^{3+} ions, the volume fraction

of magnetic shielding at $10\,\mathrm{K}$ was estimated to be over 50%, indicating bulk superconductivity. The differential χ_{FC} curve in the inset of fig. 5 shows that the T_c^{onset} is over $56\,\mathrm{K}$, consistent with the resistance measurement. Therefore, Th-doping in GdFeAsO elevates the T_c by $20\,\mathrm{K}$ and $2.5\,\mathrm{K}$, respectively, compared with $GdO_{0.83}F_{0.17}FeAs$ [11] and high-pressure synthesized $GdFeAsO_{1-x}$ [16]. To our knowledge, this value of T_c^{onset} is among the highest ever discovered in iron-based oxypnictides.

Our observation of superconductivity in $Gd_{1-x}Th_xFeAsO$ indicates that the Ln-site substitution in LnFeAsO is feasible to realize electron doping, hence the high-temperature superconductivity. Moreover, the electron-doping is more easily induced by the Th^{4+}-substitution compared with the F^--substitution in GdFeAsO. It is thus expected that the thorium-doping strategy can be applied to other iron-based oxypnictides.

$$* * *$$

REFERENCES

[1] Kamihara Y. *et al.*, *J. Am. Chem. Soc.*, **130** (2008) 3296.
[2] Takahashi H. *et al.*, *Nature*, **453** (2008) 376.
[3] Chen X. H. *et al.*, *Nature*, **354** (2008) 761.
[4] Chen G. F. *et al.*, *Phys. Rev. Lett.*, **100** (2008) 247002.
[5] Ren Z. A. *et al.*, *Europhys. Lett.*, **82** (2008) 57002.
[6] Ren Z. A. *et al.*, cond-mat/0803.4283 (2008).
[7] Ren Z. A. *et al.*, *Chin. Phys. Lett.*, **25** (2008) 2215.
[8] Liu R. H. *et al.*, cond-mat/0804.2105v3 (2008).
[9] Ren Z. A. *et al.*, *Europhys. Lett.*, **83** (2008) 17002.
[10] Chen G. F. *et al.*, *Chin. Phys. Lett.*, **25** (2008) 2235.
[11] Cheng P. *et al.*, *Sci. China G*, **51** (2008) 719.
[12] Quebe P., Terbuchte L. J. and Jeitschko W., *J. Alloys Compd.*, **302** (2000) 70.
[13] Johnson V. and Jeitschko W. J., *Solid State Chem.*, **11** (1974) 161.
[14] Shannon R. D., *Acta Crystallogr., Sect. A*, **32** (1976) 751.
[15] Cava R. J., *J. Am. Ceram. Soc.*, **83** (2000) 5.
[16] Yang J. *et al.*, *Supercond. Sci. Technol.*, **21** (2008) 082001.
[17] Wen H. H. *et al.*, *Europhys. Lett.*, **82** (2008) 17009.
[18] Tokura Y., Takagi H. and Uchida S., *Nature*, **337** (1989) 345.
[19] Dong J. *et al.*, *Europhys. Lett.*, **83** (2008) 27006.
[20] Cruz C. *et al.*, *Nature*, **453** (2008) 899.
[21] Nomura T. *et al.*, cond-mat/0804.3569v1 (2008).
[22] Ding L. *et al.*, *Phys. Rev. B*, **77** (2008) 180510R.